Supporting Information

Epitaxial Growth of Hexahedral Fe_2O_3@SnO_2 Nano Heterostructure for Improved Lithium-Ion Battery

Xiong Wang [a], Rui Wang [a]*, Qiaoling Kang [a]*, Feng Gao [b], Miaogen Chen [d], Yang Xu [a], Hongliang Ge [ac], Dongyun Li [ac]*

a College of Materials and Chemistry, China Jiliang University, Hangzhou, 310018, China.

b Department of Materials Science and Engineering, Jiangsu Key Laboratory of Artificial Functional Materials, Collaborative Innovation Center of Advanced Microstructures, College of Engineering and Applied Sciences, Nanjing University, Nanjing 210023, PR China.

c Magnetism Key Laboratory of Zhejiang Province, China Jiliang University, Hangzhou 310018, China

d Department of Physics, China Jiliang University, Hangzhou 310018, PR China

*Corresponding Authors:

E-mail: wangrui@cjlu.edu.cn E-mail: kangqiaoling@cjlu.edu.cn

E-mail: lidongyun@cjlu.edu.cn

Content

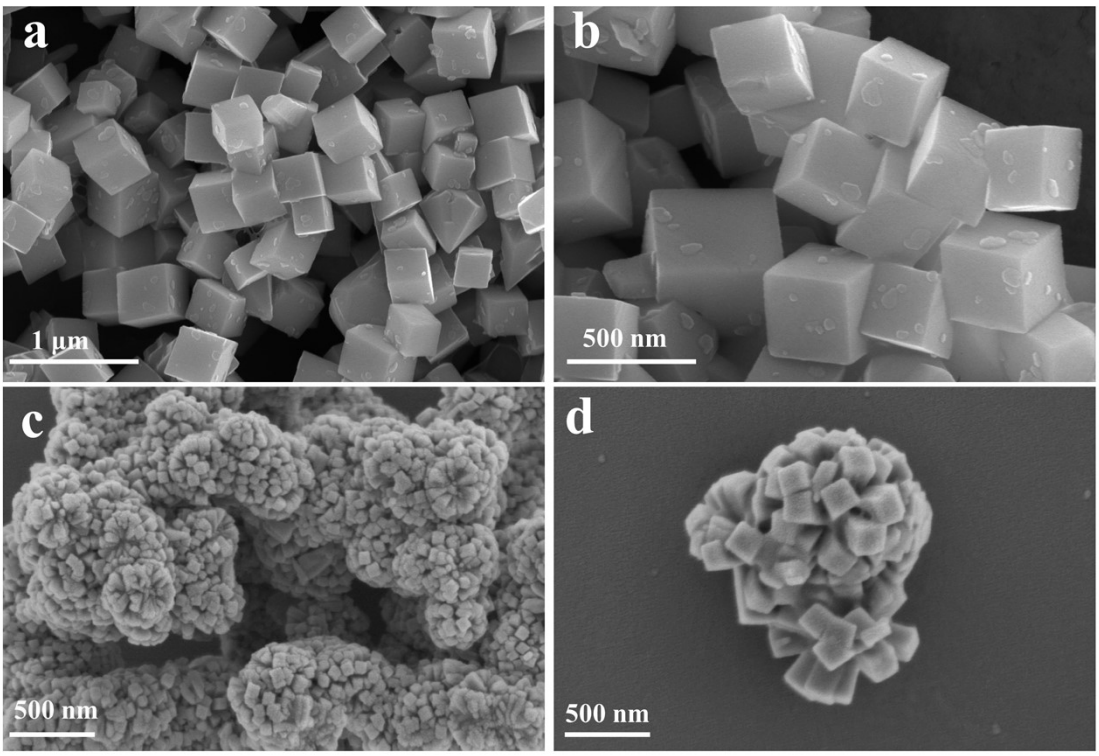

Fig. S1. SEM images of (a-b) hexahedral Fe_2O_3 cubes; (c-d) SnO_2 nanopillars

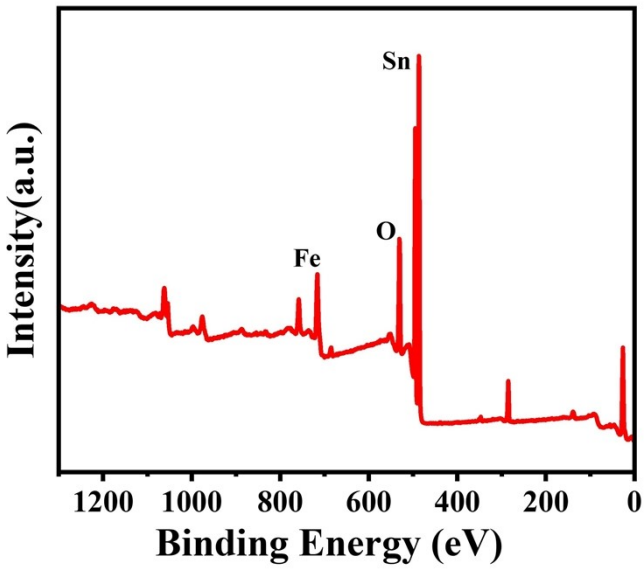

Fig. S2. The survey spectra of the hexahedral Fe_2O_3@SnO_2 heterostructure.

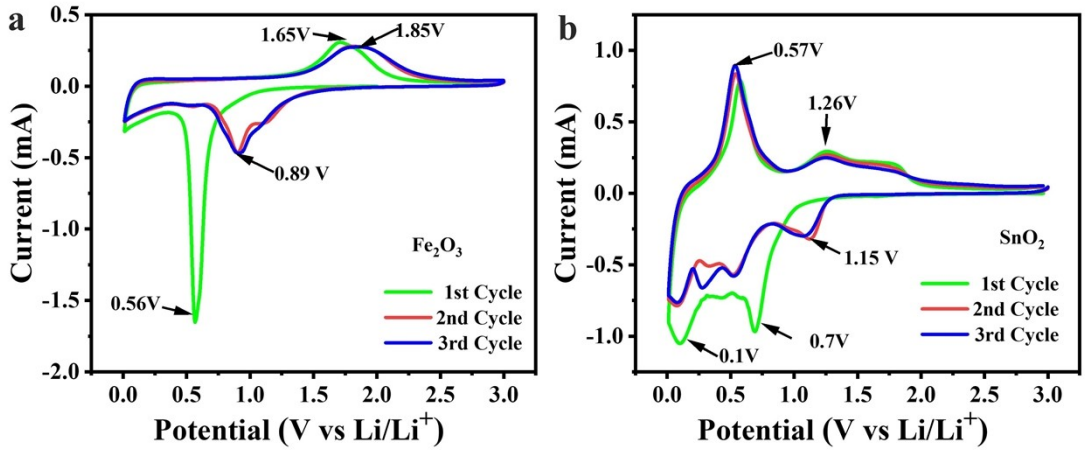

Fig. S3. CV curves of initial three cycles at scan rate 0.1 mV s^{-1} of (a) hexahedral Fe_2O_3 heterostructure;(b) SnO_2 nanopillars.

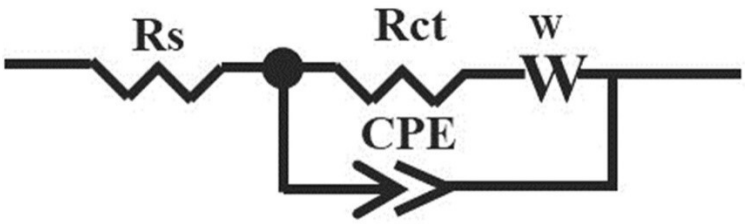

Fig. S4. The equivalent circuit of the three samples.

Table S1. Key parameters in the mechanical and electrochemical simulations.

Parameter	Value	Unit	Definition
T_{ref}	293.15	K	Reference temperature
α_{fs}	12.3E-5	K^{-1}	Thermal expansion coefficient of Fe_2O_3
ρ_{fs}	2.33	g cm^{-3}	Density of Fe_2O_3
E_{fs}	140E-9	Pa	Young's modulus of Fe_2O_3
ν_{fs}	0.256	1	Poisson's ratio of Fe_2O_3

Table S2. Hexahedral Fe_2O_3@SnO_2 heterostructure and other Fe-based anode reported in other recent literatures are used to LIBs' anode.

Material system	Specific Capacity	Reference
Fe_2O_3@SnO_2	**641.7 mAh g^{-1}@4 Ag^{-1}**	**This work**
H-Co_3O_4@MCNBs	658 mAh g^{-1} @2 A g^{-1}	Angew. Chem. Int. Ed. 59(45) (2020) 19914-19918.
Co_3O_4@MnO_2	696 mAh g^{-1}@1 A g^{-1}	Small 17(19) (2021) 9. 2008165.
SF	558.3 mAh g^{-1} @5 A g^{-1}	Chem. Eng. J. 388 (2020) 8. 124119.
α-MoO_3/SWCNH	654mAh g^{-1} @1C	Adv. Energy Mater. 10(36) (2020) 14. 2001627.
d-H-Nb_2O_5	138mAh g^{-1} @2 A g^{-1}	Energy Environ. Sci. 15(1) (2022) 254-264.
SnO_2@MOF/graphene	450 mAh g^{-1} @1 A g^{-1}	Nano Energy 74 (2020) 10. 104868.
$HoCo_3O_4$/NS-RGO	820 mAh g^{-1} @5 A g^{-1}	ACS Nano 14(5) (2020) 5780-5787.
V_2O_5	318 mA h g^{-1} @3 A g^{-1}	Nano Energy 78 (2020) 10. 105233.
LBL	206 mAh g^{-1} @4 A g^{-1}	Energy Stor. Mater. 38 (2021) 70-79.

Table S3. Formula form of strain and stress of electrochemical and thermal models.

	Strain	Stress
Electrochemical model	$\varepsilon_e = \beta(I-I_{ref}) = \beta\Delta I$ [1]	$\sigma_t = E_e\beta\Delta I$ [2]
Thermal model	$\varepsilon_t = \alpha(T-T_{ref}) = \alpha\Delta T$ [3]	$\sigma_t = E_t\alpha\Delta T$ [4]

Reference

[1] H. Yang, F. F. Fan, W. T. Liang, X. Guo, T. Zhu, S. L. Zhang, A chemo-mechanical model of lithiation in silicon, J. Mech. Phys. Solids 70 (2014) 349-361. https://doi.org/10.1016/j.jmps.2014.06.004.

[2] H. M. Xie, Q. Zhang, H. B. Song, B. Q. Shi, Y. L. Kang, Modeling and in situ characterization of lithiation-induced stress in electrodes during the coupled mechano-electro-chemical process, J. Power Sources 342 (2017) 896-903. https://doi.org/10.1016/j.jpowsour.2017.01.017.

[3] M. Wang, X. R. Xiao, Investigation of the chemo-mechanical coupling in lithiation/delithiation of amorphous Si through simulations of Si thin films and Si nanospheres, J. Power Sources 326 (2016) 365-376. https://doi.org/10.1016/j.jpowsour.2016.07.011.

[4] D. A. Cui, M. J. Cheng, Thermal stress modeling of anode supported micro-tubular solid oxide fuel cell, J. Power Sources 192(2) (2009) 400-407. https://doi.org/10.1016/j.jpowsour.2009.03.046.